



# Quantitative Assessment of DECT Perfusion Parameters in Acute Pulmonary Embolism: Association with CT-Based Severity Indices

Necat Islamoğlu<sup>1,\*</sup>, Ali Sami Kıvrak<sup>2</sup>, Fikret Kanat<sup>3</sup>, Seda Ozbek<sup>2</sup>

<sup>1</sup> Konya City Hospital, Konya, Turkey

<sup>2</sup> Department of Radiology, Selcuk University Faculty of Medicine, Konya, Turkey

<sup>3</sup> Department of Chest Diseases, Selcuk University Faculty of Medicine, Konya, Turkiye

\*Corresponding Author: Konya City Hospital, Konya, Turkey. Email: nislamoglu@yahoo.com

Received: 24 January, 2026; Revised: 16 February, 2026; Accepted: 27 February, 2026

## Abstract

**Background:** Acute pulmonary embolism (PE) is a clinically serious and potentially fatal condition that requires rapid diagnosis and accurate assessment of disease severity. Although computed tomography angiography (CTA) is the primary imaging modality for detecting emboli, it mainly provides morphological information and does not directly assess pulmonary perfusion. Dual-energy computed tomography (DECT) enables simultaneous anatomical and perfusion imaging using iodine mapping.

**Objectives:** This study aimed to evaluate the association between DECT-derived perfusion parameters and established CT-based severity indices, including the perfusion defect score and perfusion defect volume (PDvol), which were quantified using dedicated dual-energy post-processing software (LungPBV, Syngo Dual Energy, Siemens Healthcare, Forchheim, Germany), in patients with acute PE. These parameters were also compared with established radiologic severity indicators, including the CTA obstruction score and the right ventricular/left ventricular (RV/LV) diameter ratio.

**Methods:** This retrospective analysis included 35 patients with confirmed acute PE from among 280 individuals who underwent DECT between June 2013 and December 2013. CTA obstruction scores were calculated using the Qanadli method. RV/LV diameter ratios were calculated on axial CTA images. Perfusion defect scores were determined using a segment-based scoring system on iodine maps. PDvol was determined semi-automatically using dedicated volumetric software. Correlations between perfusion parameters and established severity markers were assessed statistically.

**Results:** The mean CTA obstruction score was  $33.7 \pm 22.4\%$ , and the mean RV/LV diameter ratio was  $1.06 \pm 0.2$ . The mean perfusion defect score was  $27.4 \pm 15.1\%$ , and the mean PDvol was  $23.8 \pm 11.8\%$ . Significant positive correlations were observed between segmental obstruction on CTA and corresponding perfusion defects ( $P < 0.001$ ). PDvol showed a statistically significant association with both the CTA obstruction score and the perfusion defect score, whereas no statistically significant association was observed between PDvol and the RV/LV ratio.

**Conclusion:** DECT perfusion imaging provides both qualitative and quantitative assessments of pulmonary perfusion abnormalities in acute PE. Quantitative assessment using PDvol correlates with the CTA obstruction score and may provide objective information regarding imaging-based disease burden.

**Keywords:** Acute Pulmonary Embolism, Dual-energy Computed Tomography, Perfusion Defect Score, Perfusion Defect Volume, RV/LV Ratio, Iodine Mapping

## 1. Background

Acute pulmonary embolism (PE) is a potentially fatal disorder that requires early diagnosis and prompt treatment. It is the third leading cause of death among cardiovascular diseases, after coronary artery disease

and stroke. The mortality rate in untreated cases ranges from 25% to 30%, whereas it decreases to approximately 5% - 8% with appropriate treatment.

In routine clinical practice, commonly used methods for the evaluation of acute PE include

Copyright © 2026, Islamoğlu et al. This open-access article is available under the Creative Commons Attribution 4.0 (CC BY 4.0) International License (<https://creativecommons.org/licenses/by/4.0/>), which allows for unrestricted use, distribution, and reproduction in any medium, provided that the original work is properly cited.

**How to Cite:** Islamoğlu N, Sami Kıvrak A, Kanat F, Ozbek S. Quantitative Assessment of DECT Perfusion Parameters in Acute Pulmonary Embolism: Association with CT-Based Severity Indices. I J Radiol. 2026;23(1):e170847. doi: <https://doi.org/10.5812/iranjradiol-170847>

electrocardiography, chest radiography, arterial blood gas analysis, and D-dimer testing. However, the clinical utility of these methods remains limited. Conventional pulmonary angiography has long been considered the gold standard for the diagnosis of PE. In a comparative study evaluating the adequacy of conventional angiography and pulmonary computed tomography angiography (CTA), Baile et al. (1) reported no significant difference between the 2 imaging modalities.

Dual-energy computed tomography (DECT) is a relatively novel imaging technique that enables detailed visualization of the pulmonary vasculature while simultaneously assessing iodine distribution within the lung parenchyma. By generating iodine maps, DECT can demonstrate pulmonary perfusion defects that are otherwise detected with conventional methods, such as radionuclide perfusion scintigraphy (2). Although previous studies have evaluated the relationship between DECT perfusion parameters and CTA-based obstruction scores, most have primarily relied on semi-quantitative approaches. The present study contributes to the existing literature by providing a combined assessment of both segment-based perfusion defect scoring and volumetric quantification (PDvol) within the same patient cohort. This integrated approach enables a more comprehensive evaluation of imaging-based severity in acute PE.

## 2. Objectives

This study aimed to evaluate pulmonary perfusion abnormalities using DECT-derived parameters and to investigate their association with established CT-based severity indices in patients with acute PE.

## 3. Patients and Methods

### 3.1. Patient Enrollment

This study was initiated after approval was obtained from the Non-Interventional Clinical Research Ethics Committee of Selçuk University Faculty of Medicine (approval number: 2013/263; date: August 20, 2013). The study was designed as a retrospective analysis of dual-energy computed tomography angiography (DECTA) examinations performed for the preliminary diagnosis of PE in the Department of Radiology.

Between June 2013 and December 2013, DECTA images of 280 patients with a preliminary diagnosis of acute PE, archived in the hospital Picture Archiving and Communication System (PACS) (Enlil PACS, Eroğlu, Eskişehir, Türkiye), were retrospectively reviewed. The

patient selection and exclusion process is summarized in [Figure 1](#).

Image evaluations were performed by 2 radiologists with experience in thoracic imaging, each with more than 5 years of experience. The first radiologist evaluated CTA images for the presence of acute PE, accompanying pathologies, CT angiographic obstruction scores, and the right ventricular to left ventricular (RV/LV) diameter ratio. The second radiologist independently evaluated perfusion abnormalities on iodine maps and was blinded to CTA findings and clinical data. This study did not include a formal assessment of interobserver variability. The primary endpoint was the correlation between PDvol and the CT angiographic obstruction score. Secondary endpoints included associations among perfusion defect score, RV/LV diameter ratio, and other imaging-based parameters. Given the retrospective design and limited sample size, all analyses were considered exploratory and hypothesis-generating.

Acute PE was diagnosed using CTA findings as the reference standard, based on the presence of intraluminal contrast filling defects within the pulmonary arterial tree. Patients without PE and those with concomitant conditions that could potentially confound perfusion assessment, such as infection, tumor, or atelectasis, were excluded. Cases with insufficient vascular opacification for definitive PE diagnosis were also excluded.

For analysis, the pulmonary arterial circulation was subdivided into 10 segmental vessels: 3 in the upper lobe, 2 in the middle lobe, and 5 in the lower lobe. In patients with confirmed acute PE, the segments containing thrombus were recorded. PE was classified as total or partial obstruction according to the degree of luminal occlusion. Total obstruction was defined as a thrombus completely occluding the lumen, with no visible contrast distal to the obstruction. Partial obstruction was defined as a central thrombus surrounded by contrast material within the lumen.

### 3.2. DECT Imaging Protocol

DECT imaging was performed using a 128-slice dual-source multidetector CT scanner (Somatom Definition Flash, Siemens Healthcare, Forchheim, Germany). Acquisition parameters were as follows: matrix size, 512 × 512; tube voltage A/B, 100/140 kV; tube current A/B, 89/76 mAs; gantry rotation time, 0.28 seconds; slice thickness, 0.625 mm; reconstruction thickness, 1 mm; pitch, 0.55; and field of view A/B, mean 38 cm/maximum 33 cm. To minimize beam-hardening artifacts caused by contrast material in the superior vena cava, CT

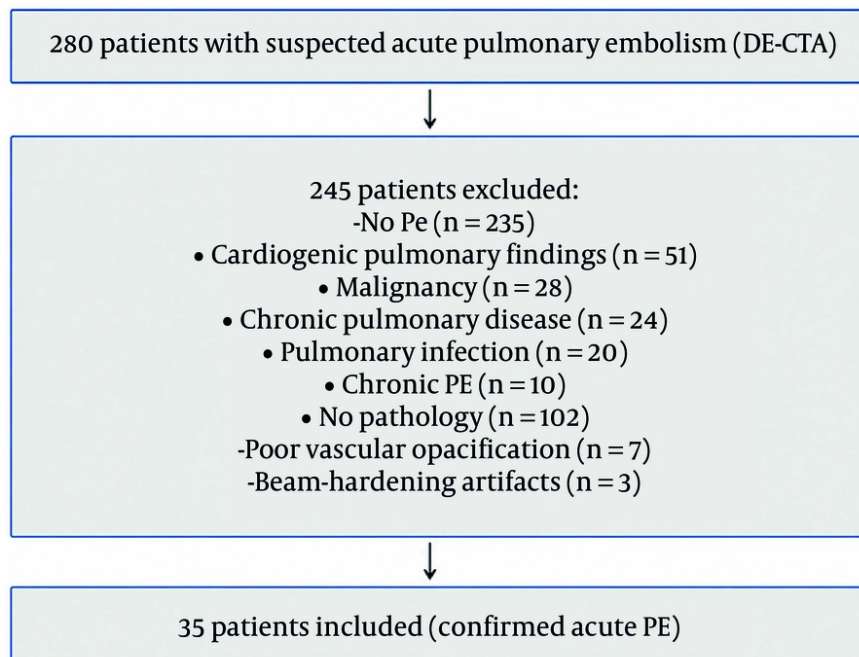


**Figure 1.** Flow diagram of patient selection and exclusion process

acquisition was performed in a caudocranial direction during a single breath-hold, covering the region from the lung bases to the apices.

All DECTA examinations were performed using a non-ionic iodinated contrast agent containing 350 mg/mL iodine (iopromide; Ultravist 350, Bayer, Berlin, Germany). Contrast material was administered via an antecubital vein using an automatic injector (Ulrich power injector, Germany) at a rate of 4.5 mL/s, followed by a 20-mL saline flush at 5 mL/s. Bolus tracking was used to achieve optimal pulmonary arterial enhancement. Before contrast injection, a monitoring region was placed at the right ventricular level, and image acquisition was triggered automatically when attenuation reached 80 Hounsfield units. The total contrast volume was determined by multiplying the injection rate (4.5 mL/s) by the sum of the scan duration and the pre-scan delay time.

Simultaneous helical acquisition was performed using tube voltages of 100 and 140 kV. Mixed images were automatically generated from the combined datasets and transferred to a dedicated post-processing Leonardo workstation (Syngo Dual Energy software, Siemens Healthcare, Forchheim, Germany) for analysis.

### 3.3. CT-Derived Parameters

#### 3.3.1. CT Angiographic Obstruction Score

The obstruction index was determined on mixed images using the Qanadli method within the dual-energy software environment. In this scoring system, n represents the number of obstructed segmental arteries, and d represents the degree of obstruction (0 = no obstruction; 1 = partial obstruction; 2 = total obstruction) (3).

#### 3.3.2. RV/LV Diameter Ratio

The RV/LV diameter ratio was assessed on axial CTA images based on previously described measurement approaches. The right ventricular short-axis diameter was obtained at the tricuspid valve level by measuring the maximum distance between the interventricular septum and the RV free wall. The left ventricular short-axis diameter was determined at the level of the mitral valve as the greatest distance between the LV free wall and the interventricular septum (Figure 2) (4).

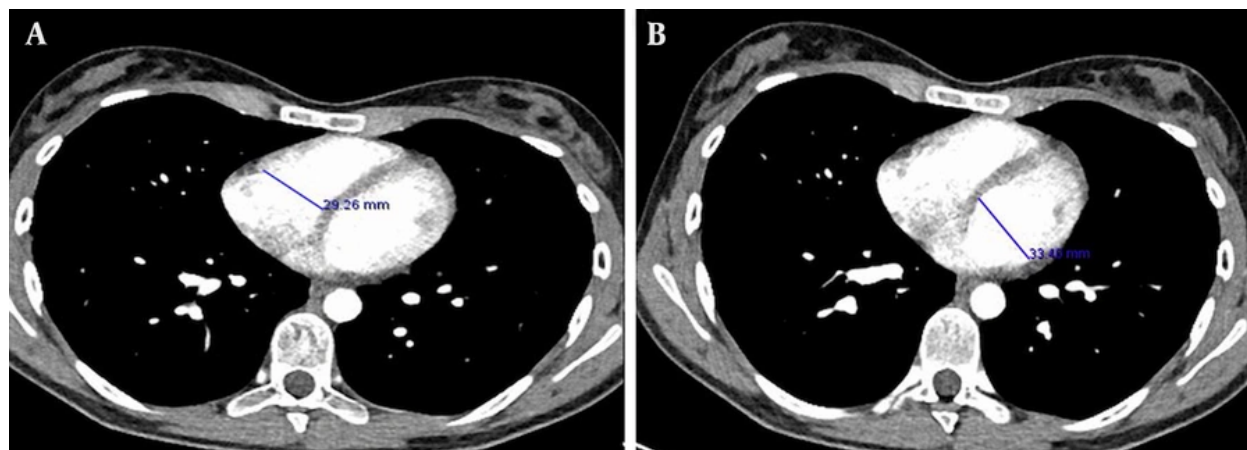


**Figure 2.** A, Right ventricular diameter measurement; B, left ventricular diameter measurement.

### 3.3.3. Perfusion Defect Score

Perfusion images were generated on the workstation separately from the CTA dataset and were interpreted independently, without access to CTA findings, to reduce interpretation bias. Each lung was divided into 10 segments, consistent with the CT angiographic obstruction scoring method.

On iodine perfusion maps, normal pulmonary perfusion, defined as a parenchymal segment without color loss, was scored as 0; moderately decreased perfusion, defined as a parenchymal segment with mild color attenuation, was scored as 1; and severely decreased or absent perfusion, defined as a segment with marked or near-complete color loss, was scored as 2 (Figure 3). The final perfusion defect score was calculated using the following formula:

$$\sum \frac{(n \times d)}{40} \times 100$$

where n represents the number of segments with perfusion defects and d represents the perfusion score of the affected segment.

### 3.3.4. Absolute Perfusion Defect Volume

PDvol was calculated using dedicated dual-energy volumetric analysis software (LungPBV, Syngo Dual Energy, Siemens Healthcare, Forchheim, Germany) on iodine map images at the workstation.

The analysis was performed in a stepwise manner. First, total lung volume was automatically calculated by the software. Second, perfusion defect areas were identified on iodine maps as regions showing reduced or absent iodine-related enhancement. Third, these regions were manually delineated on each axial image slice by contouring the areas corresponding to perfusion abnormalities (Figure 4). The software then calculated the total perfusion defect volume.

PDvol was expressed as a percentage of total lung volume using the following formula:

$$\text{PDvol (\%)} = (\text{defect volume} / \text{total lung volume}) \times 100$$

To minimize false-positive findings, areas affected by beam-hardening artifacts, particularly those related to contrast material in the superior vena cava, were carefully evaluated and excluded from the analysis.

### 3.4. Statistical Analysis

All data were transferred to a computerized database and checked for potential entry errors. Statistical analyses were performed using SPSS version 15.0 (SPSS Inc., Chicago, IL, USA). Continuous variables were expressed as mean  $\pm$  standard deviation.

Normality assumptions for continuous variables were assessed using visual methods, including histograms and Q-Q plots. Given the non-parametric nature of the variables and the sample size, relationships among the CT angiographic obstruction

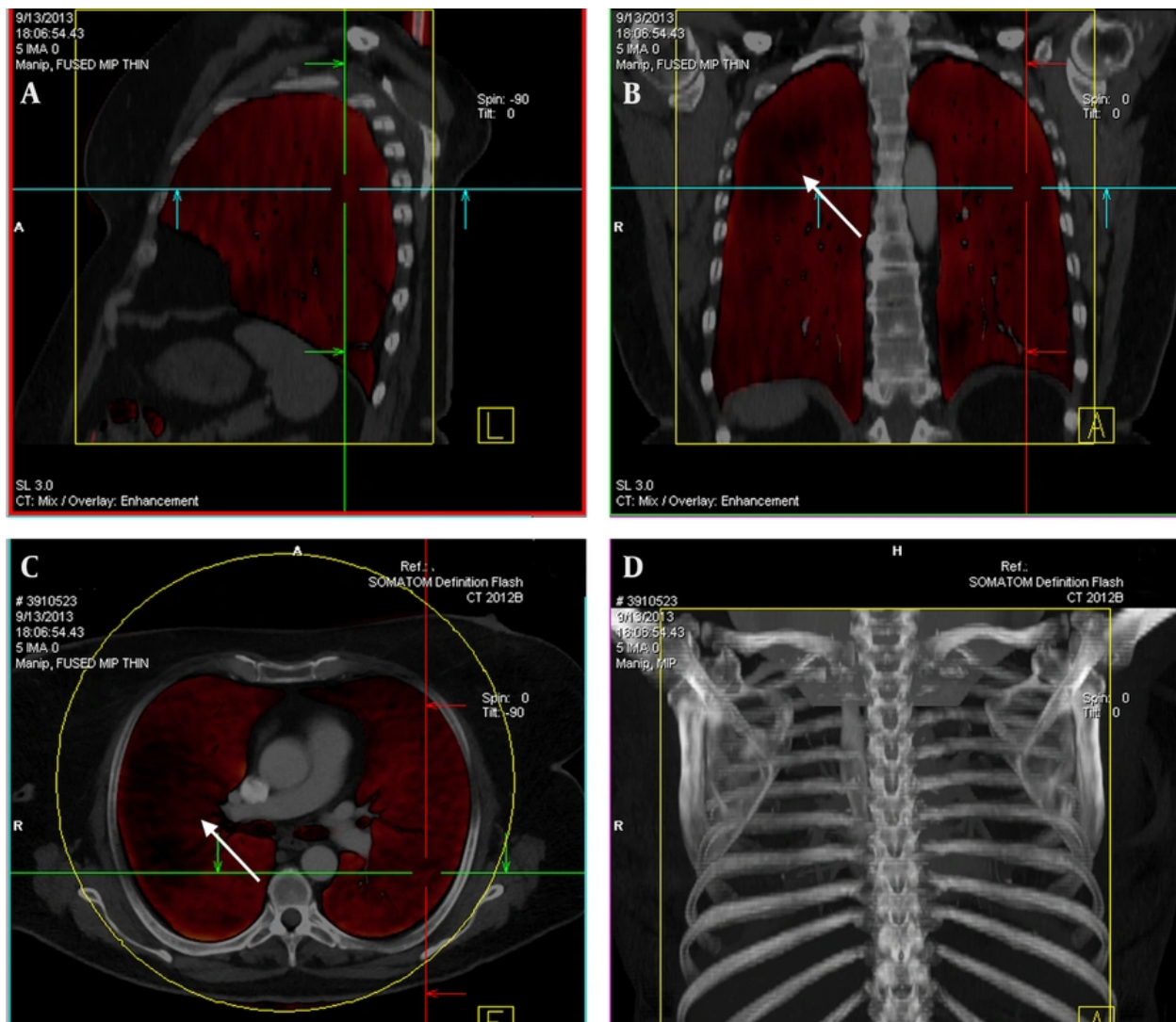


**Figure 3.** A, sagittal; B, coronal, and C, axial dual-energy CT iodine perfusion maps demonstrating a complete perfusion defect in the right upper lobe segment (arrows; defect score = 2). D, Corresponding 3-dimensional reconstruction image.

score, RV/LV diameter ratio, perfusion defect score, and perfusion defect volume were evaluated using Spearman rank correlation analysis. Spearman correlation coefficients ( $r_s$ ) were reported with 95% confidence intervals (CIs) and exact P values. Statistical significance was defined as  $P < 0.05$ . Because the analyses were exploratory and the number of comparisons was limited, no formal adjustment for multiple comparisons was performed.

**4. Results**

A total of 280 patients who underwent DECTA for suspected acute PE were initially reviewed. Of these, 35 (12.5%) were diagnosed with acute PE and included in the final analysis. The remaining 245 patients were excluded for the following reasons: 235 did not meet the diagnostic criteria for acute PE, including cardiogenic pulmonary findings ( $n = 51$ ), malignancy ( $n = 28$ ), chronic pulmonary disease ( $n = 24$ ), pulmonary infection ( $n = 20$ ), chronic PE ( $n = 10$ ), and absence of pathology ( $n = 102$ ). In addition, 7 patients were excluded because of insufficient vascular opacification,

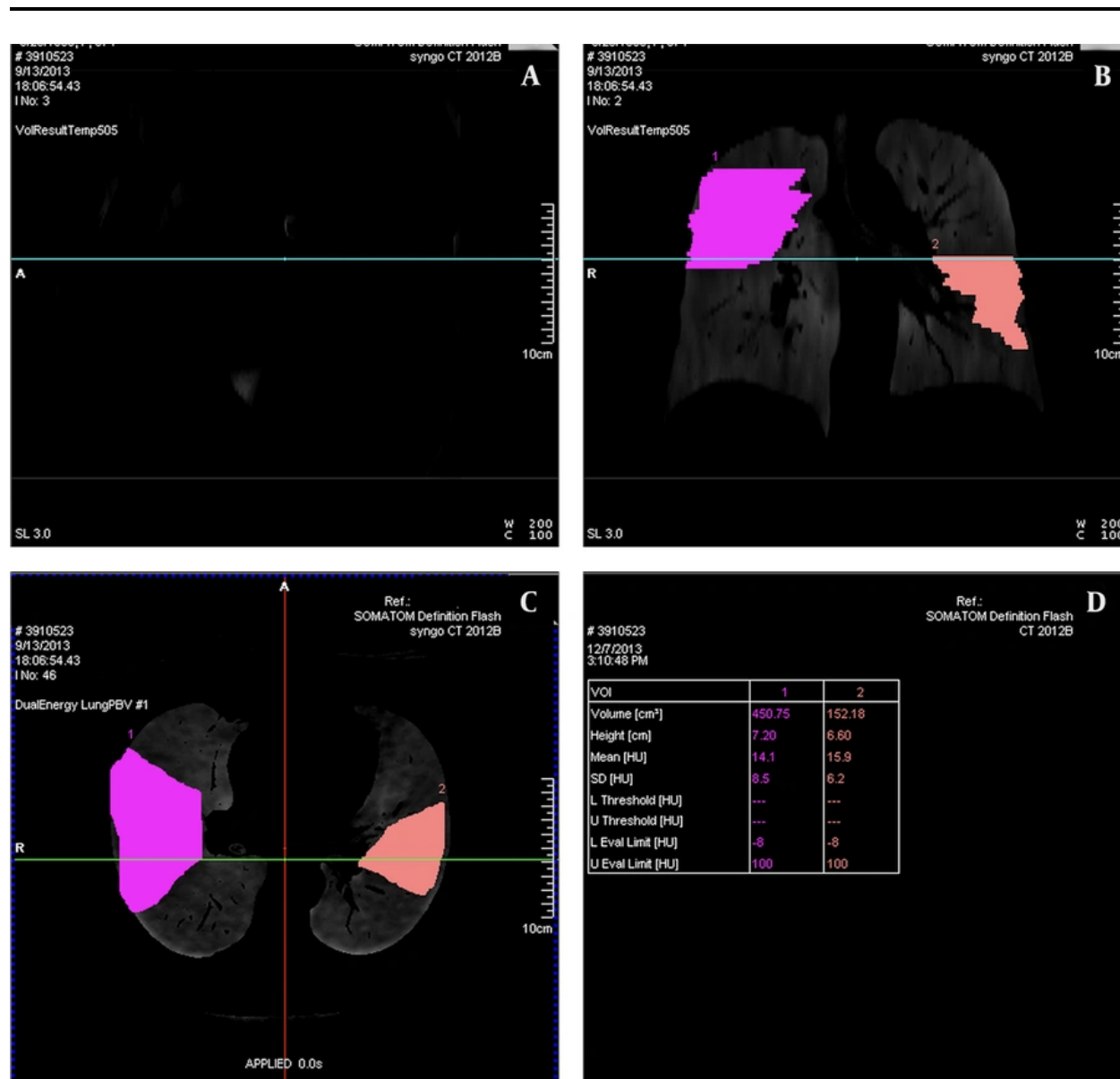


**Figure 4.** A, Sagittal; B, coronal, and C, axial iodine map images demonstrating semi-automated segmentation of perfusion defect areas. D, Quantitative volumetric analysis generated by the LungPBV software.

and 3 were excluded because of beam-hardening artifacts that caused pseudo-perfusion defects (Figure 1).

Of the 35 patients included in the study, 22 (62%) were male and 13 (38%) were female. Patient age ranged from 26 to 89 years, with a mean age of 62.5 ± 16.7 years. Among these 35 patients with confirmed acute PE, 8 demonstrated only partial obstruction, 5 demonstrated only total obstruction, and 22 demonstrated both total

and partial obstruction. Right-sided PE was present in 14 patients (40%), left-sided PE in 2 patients (6%), and bilateral PE in 19 patients (54%).

Regarding embolus distribution, 36.8% were located in the right lower lobe, 24.8% in the left lower lobe, 15.2% in the right upper lobe, 8.5% in the right middle lobe, 7.8% in the left middle lobe, and 6.9% in the left upper lobe.

CT angiographic measurements revealed obstruction scores ranging from 2.5% to 75%, with a mean obstruction score of  $33.7 \pm 22.4\%$ . The right ventricular diameter ranged from 22.5 mm to 55 mm, with a mean of  $38.9 \pm 7.2$  mm. The left ventricular diameter ranged from 25 mm to 49.8 mm, with a mean of  $37 \pm 6.3$  mm. The RV/LV diameter ratio ranged from 0.6 to 1.6, with a mean of  $1.06 \pm 0.2$  (Table 1).

**Table 1.** Computed Tomography Pulmonary Angiography Obstruction Score, RV, LV, and RV/LV Ratio Values<sup>a</sup>

Variables	Minimum-maximum	Mean $\pm$ SD
Obstruction score (%)	2.5 - 75	33.7 $\pm$ 22.4
RV (mm)	22.5 - 55	38.9 $\pm$ 7.2
LV (mm)	25 - 49.8	37 $\pm$ 6.3
RV/LV ratio	0.6 - 1.6	1.06 $\pm$ 0.2

<sup>a</sup> Abbreviations: LV, left ventricle; RV, right ventricle. RV and LV are expressed in millimeters. RV/LV represents a unitless ratio.

Based on iodine perfusion maps generated at the workstation, the perfusion defect score ranged from 5% to 67.5%, with a mean of  $27.4 \pm 15.1\%$ . Total lung volume ranged from 1708 mL to 5274 mL, with a mean of  $2740 \pm 1109$  mL. Perfusion defect volume ranged from 92.5 mL to 1842 mL, with a mean of  $636 \pm 420$  mL. PDvol ranged from 3% to 50.3%, with a mean of  $23.8 \pm 11.8\%$  (Table 2).

**Table 2.** Perfusion Defect Score, Total Lung Volume, Perfusion Defect Volume, and Absolute Perfusion Defect Volume Values<sup>a</sup>

Variables	Minimum-maximum	Mean $\pm$ SD
Perfusion defect score (%)	5 - 67.5	27.4 $\pm$ 15
Total lung volume (mL)	1708 - 5274	2740 $\pm$ 1109
Perfusion defect volume (mL)	92.5 - 1842	636 $\pm$ 420
PDvol (%)	3 - 50.3	23.8 $\pm$ 12

<sup>a</sup> Abbreviations: PDvol, perfusion defect volume. PDvol represents the percentage of total lung volume affected by perfusion defects.

In accordance with the primary study objective, statistical analysis demonstrated a significant positive correlation between the total number of segments showing partial obstruction on CTA and the number of segments with partial perfusion defects on perfusion mapping ( $r_s = 0.618$ ; 95% CI, 0.35 - 0.79;  $P < 0.001$ ). Similarly, a strong positive correlation was observed between the total number of segments with total obstruction on CTA and the number of segments with total perfusion defects ( $r_s = 0.772$ ; 95% CI, 0.55 - 0.88;  $P < 0.001$ ). Detailed correlation analyses are presented in Table 3.

**Table 3.** Correlation Analysis Between CT Angiographic Obstruction Findings and Perfusion Abnormalities<sup>a</sup>

Variables Compared	Spearman $r_s$	95% CI	P-value
Partial obstruction vs partial perfusion	0.618	0.35 - 0.79	< 0.001
Total obstruction vs total perfusion	0.772	0.55 - 0.88	< 0.001

<sup>a</sup> Values are presented as Spearman correlation coefficients ( $r_s$ ) with 95% confidence intervals.

## 5. Discussion

In recent decades, pulmonary CTA has emerged as the first-line imaging modality for diagnosing acute PE. However, concerns have been raised regarding the potential overuse of CT pulmonary angiography in clinical practice, underscoring the importance of appropriate patient selection and imaging strategies (5). Compared with conventional pulmonary angiography, CTA is minimally invasive and enables direct visualization of emboli while also providing additional information on lung parenchymal, mediastinal, pleural, and chest wall pathologies. Another advantage of CTA is its utility in monitoring treatment response. Advances in detector technology have shortened acquisition times and facilitated the widespread use of multidetector CT. This has improved visualization of small pulmonary arteries and detection of subsegmental emboli. Consequently, CTA has become the primary imaging technique for evaluating the pulmonary vasculature in patients with suspected PE (6, 7).

Acute PE can lead to pulmonary hypertension, causing the right ventricle to pump blood against increased resistance. As a result, right ventricular dilation and dysfunction may occur, leading to reduced cardiac output. Enlargement of the right ventricle and decreased left ventricular pressure may cause leftward deviation of the interventricular septum (8). Particularly in submassive PE, right ventricular dilation has been shown to be associated with an increased risk of early mortality (9). Under physiological conditions, the RV diameter is equal to or smaller than the LV diameter. However, in acute PE with right ventricular dysfunction, increased RV pressure leads to an elevated RV/LV diameter ratio (4). Park et al. (10), in a retrospective analysis comparing echocardiography and CTA findings in patients with PE, demonstrated that an RV/LV ratio greater than 1 is a reliable indicator of right ventricular dysfunction.

Although pulmonary CTA is the primary imaging method for detecting acute PE, it provides only morphological information on vascular occlusion and

does not offer a functional assessment of pulmonary perfusion. Ventilation-perfusion scintigraphy remains a frequently used method for evaluating lung perfusion (11). Although ventilation-perfusion scintigraphy has high sensitivity for acute PE, its specificity is relatively low. Furthermore, it cannot accurately determine the degree of obstruction or identify the underlying causes of perfusion loss, limiting its clinical utility compared with CTA (12).

With advancements in CT technology, dual-energy acquisition has enabled simultaneous volumetric data acquisition at 2 energy levels. The development of DECTA has made it possible to obtain both morphological and functional information in a single examination (10). Thoracic DECTA applications include perfusion imaging in PE, xenon ventilation-perfusion imaging, and characterization of solitary pulmonary nodules (13, 14).

DECTA allows the generation of iodine maps, enabling detection of pulmonary perfusion defects similar to those demonstrated by radionuclide perfusion scintigraphy (2). Earlier studies have shown that DECTA can identify perfusion defects secondary to embolism in patients with acute PE (4, 15-17).

Zhang et al. (18) reported that perfusion defect volume alone demonstrated a sensitivity of 87% and specificity of 98% for detecting acute PE in histopathologically confirmed cases. In the same study, CTA demonstrated a sensitivity of 67% and specificity of 100%. Zhou et al. (9) demonstrated a strong correlation between CTA obstruction scores and perfusion defect scores. In contrast, Hoey et al. (19) did not find a statistically significant association between DECT perfusion defect scores and CTA obstruction scores in patients with chronic PE. Discrepancies between obstruction scores and perfusion-based measurements may be attributable to preserved perfusion in partially occluded segments (20). Chung et al. (21) demonstrated that CTA detects more lesions in cases of large emboli, whereas perfusion imaging may be more sensitive for detecting smaller emboli. Perfusion defects that appear more extensive than vascular obstruction may reflect microvascular occlusions obscured by partial volume effects (4).

In earlier studies by Bauer et al. (16) and Chae et al. (4), perfusion defect scores derived from DECTA were compared with CTA obstruction scores and RV/LV diameter ratios to assess the extent of acute PE. These studies demonstrated significant correlations among perfusion defect score, RV/LV ratio, and CTA obstruction score. However, perfusion defects were not quantified

volumetrically, and the findings were not evaluated using fully quantitative methods.

Apfaltrer et al. (20) compared the RV/LV diameter ratio, RV/LV volume ratio, and CTA obstruction score, calculated using the Qanadli method, with clinical severity in acute PE and found significant correlations. They also demonstrated that PDvol had the strongest association with both clinical severity and CTA obstruction score. In their study, no statistically significant association was observed between PDvol and RV/LV ratio.

In the present study, a statistically significant association was observed between perfusion defect score and CTA obstruction score; however, no statistically significant association was found between perfusion defect score and RV/LV ratio. When patients were stratified according to RV/LV ratio ( $> 1$  vs  $\leq 1$ ), the group with an RV/LV ratio greater than 1 demonstrated a 13% higher mean CTA obstruction score and a 6.3% higher mean perfusion defect score. Additionally, all evaluated parameters were higher in the group with an RV/LV ratio greater than 1.

Consistent with the literature, a statistically significant association was observed between segments showing partial and total obstruction on CTA and segments demonstrating partial and total perfusion defects on iodine maps.

In the limited number of studies evaluating PDvol derived from iodine maps, Apfaltrer et al. (20) reported that PDvol was the parameter most strongly correlated with both clinical severity and CTA obstruction score. In the present study, PDvol demonstrated significant correlations with perfusion defect volume, perfusion defect score, and CTA obstruction score, consistent with previous findings. These findings indicate that PDvol, obtained through semi-automated quantitative analysis, may provide a more objective quantitative measure than a subjective perfusion defect scoring system. Similar to the findings of Apfaltrer et al. (20), no statistically significant association was observed between PDvol and RV/LV ratio in the present study.

### 5.1. Limitations

This study has several inherent limitations. First, parameters obtained from DECT perfusion imaging were not correlated with clinical severity indicators, such as the Pulmonary Embolism Severity Index or simplified Pulmonary Embolism Severity Index scores, cardiac biomarkers such as troponin or B-type natriuretic peptide, oxygen saturation, or hemodynamic parameters. Therefore, the present study is limited to imaging-based associations and does not

allow direct assessment of clinical severity or prognostic implications.

Second, potential confounding conditions that may affect pulmonary perfusion or the RV/LV ratio, such as chronic pulmonary hypertension, heart failure, or structural cardiac disease, were not systematically evaluated. These factors may influence both perfusion patterns and ventricular measurements, potentially affecting interpretation of the imaging findings. Third, possible pseudo-perfusion defects related to respiratory motion artifacts were not specifically addressed. In addition, this study lacked a formal interobserver variability analysis. The absence of a reproducibility assessment using statistical measures, such as the intraclass correlation coefficient or kappa statistics, may limit the reliability and generalizability of the imaging measurements.

Another important limitation is the use of CTA both as the reference standard for the diagnosis of acute PE and for the calculation of the CTA obstruction score, which was subsequently correlated with DECT-derived parameters. This approach may introduce incorporation bias, as the reference measurement is derived from the same imaging modality, potentially leading to overestimation of the observed associations. The relatively small sample size may limit the statistical power of the study and the generalizability of the findings. Due to the retrospective design and the limited number of eligible patients, a formal sample size calculation or power analysis was not performed, and the results should therefore be interpreted with caution. Finally, perfusion defect score and PDvol were compared only with radiologic severity parameters and were not analyzed in relation to clinical outcomes. Therefore, these parameters should be interpreted as imaging-based markers rather than direct indicators of clinical severity.

## 5.2. Conclusions

In conclusion, perfusion defect score and PDvol values obtained from DECTA perfusion imaging were compared with established CT-based parameters associated with imaging severity, including CTA obstruction score and RV/LV diameter ratio. The findings indicate that both perfusion defect score and PDvol may provide objective information related to imaging-based severity in acute PE. Quantitative assessment using PDvol may provide additional information regarding the extent of perfusion abnormalities and imaging-based disease burden.

## Footnotes

**AI Use Disclosure:** The authors declare that no generative AI tools were used in the creation of this article.

**Authors' Contributions:** N. İ., A. S. K., F. K., and S. Ö. contributed to the study concept and design and critically reviewed the manuscript for important intellectual content. N. İ. and A. S. K. contributed to data acquisition, analysis, or interpretation and drafted the manuscript. A. S. K. and S. Ö. supervised the study. All authors reviewed the final version to be published and agreed to be accountable for all aspects of the work.

**Conflict of Interests Statement:** The authors do not declare any conflicts of interests for this study.

**Data Availability:** The dataset presented in the study is available on request from the corresponding author during submission or after publication. The data are not publicly available due to privacy

**Ethical Approval:** This study was initiated following approval from the Non-Interventional Clinical Research Ethics Committee of Selçuk University Faculty of Medicine (approval number: 2013/263; date: August 20, 2013).

**Funding/Support:** No funding was received for this study.

**Informed Consent:** Informed consent was waived due to the retrospective design of the study.

**Trial Registration:** Not applicable due to the retrospective design of the study.

## References

1. Baile EM, King GG, Müller NL, D'yachkova Y, Coche EE, Paré PD, et al. Spiral computed tomography is comparable to angiography for the diagnosis of pulmonary embolism. *Am J Respir Crit Care Med*. 2000;**161**(3 Pt 1):1010-1015. [PubMed ID: [10712356](https://pubmed.ncbi.nlm.nih.gov/10712356/)]. <https://doi.org/10.1164/ajrccm.161.3.9904067>.
2. Thieme SF, Graute V, Nikolaou K, et al. Dual-energy CT lung perfusion imaging: correlation with SPECT/CT. *Eur J Radiol*. 2010;**81**(2):360-365.
3. Qanadli SD, El Hajjam M, Vieillard-Baron A, Joseph T, Mesurolle B, Oliva VL, et al. New CT index to quantify arterial obstruction in pulmonary embolism. *AJR Am J Roentgenol*. 2001;**176**(6):1415-1420. <https://doi.org/10.2214/ajr.176.6.1761415>.
4. Chae EJ, Seo JB, Jang YM, et al. Dual-energy CT for assessment of the severity of acute pulmonary embolism. *AJR Am J Roentgenol*. 2010;**194**(3):604-610.
5. Alemi H, Khoshbakht SB, Paknejad O. Avoidable overuse of computed tomography pulmonary angiography (CTPA) in patients with suspected acute pulmonary thromboembolism (PTE): the role of

- clinical prediction rules and D-dimer assay. *Shiraz E-Med J*. 2024;**25**(6). <https://doi.org/10.5812/semj-141211>.
6. Stein PD. *Pulmonary embolism*. Oxford: Wiley-Blackwell; 2007. <https://doi.org/10.1002/9780470692042>.
  7. Gupta A, Frazer CK, Ferguson JM, Kumar AB, Davis SJ, Fallon MJ, et al. Acute pulmonary embolism: diagnosis with MR angiography. *Radiology*. 1999;**210**(2):353-359. [PubMed ID: 10207414]. <https://doi.org/10.1148/radiology.210.2.r99fe53353>.
  8. Wood KE. Major pulmonary embolism: review of a pathophysiologic approach. *Chest*. 2002;**121**(3):877-905.
  9. Zhou Y, Shi H, Wang Y, et al. Assessment of correlation between CT angiographic clot load score and perfusion defect score. *Br J Radiol*. 2012;**85**(1013):972-979.
  10. Park JR, Chang SA, Jang SY, No HJ, Park SJ, Choi SH, et al. Evaluation of right ventricular dysfunction and prediction of clinical outcomes in acute pulmonary embolism by chest computed tomography: comparisons with echocardiography. *Int J Cardiovasc Imaging*. 2012;**28**(4):979-987. [PubMed ID: 21717126]. <https://doi.org/10.1007/s10554-011-9912-4>.
  11. Van Rossum AB, Treurniet FEE, Kieft GJ, et al. Role of spiral CT in patients with suspected pulmonary embolism. *Thorax*. 1996;**51**(1):23-28.
  12. Reinartz P, Wildberger JE, Schaefer W, et al. Comparison between V/Q SPECT and multislice CT. *J Nucl Med*. 2004;**45**(9):1501-1508.
  13. Karcaaltincaba M, Aktas A. Dual-energy CT revisited with multidetector CT. *Diagn Interv Radiol*. 2011;**17**(3):181-194.
  14. Turkoglu S, Özgökçe M. Effectiveness of Twin-Beam Dual-Energy Computed Tomography in Characterization of Solitary Pulmonary Nodules Larger Than 5 mm. *I J Radiol*. 2024;**21**(3). e149360. <https://doi.org/10.5812/iranjradiol-149360>.
  15. Lee CW, Seo JB, Song JW, et al. Detection of peripheral pulmonary embolism on dual-energy CT angiography. *Eur Radiol*. 2011;**21**(1):54-62.
  16. Bauer RW, Frellesen C, Renker M, et al. Dual-energy CT pulmonary blood volume assessment in acute pulmonary embolism. *Eur Radiol*. 2011;**21**(9):1914-1921.
  17. Gorgos A, Remy-Jardin M, Duhamel A, et al. Evaluation of peripheral pulmonary arteries using dual-energy CT. *J Comput Assist Tomogr*. 2009;**33**(6):981-986.
  18. Zhang LJ, Zhao YE, Wu SY, et al. Pulmonary embolism detection with dual-energy CT. *Radiology*. 2009;**252**(1):61-70.
  19. Hoey ET, Mirsadraee S, Pepke-Zaba J, et al. Dual-energy CT angiography in chronic thromboembolic pulmonary hypertension. *AJR Am J Roentgenol*. 2011;**196**(3):524-532.
  20. Apfaltrer P, Bachmann V, Meyer M, et al. Relationship between dual-energy CT perfusion parameters and clinical severity in acute pulmonary embolism. *Eur J Radiol*. 2012;**81**(11):3592-3597.
  21. Chung MJ, Goo JM, Im JG, et al. CT perfusion imaging of the lung in pulmonary embolism. *Invest Radiol*. 2004;**39**(10):633-640.